The simulation of application of high transmittance AttPSM for sub-100 nm pattern in 248 nm lithography

Cheng-ming Lin, Wen-an Loong*

Institute of Applied Chemistry, National Chiao Tung University, Hsinchu 300-10, Taiwan, ROC

Abstract

In contrast to the normal transmittance ($T < 10\%$) attenuated phase-shifting mask (AttPSM), the high transmittance AttPSM assisted with Cr scattering bars could enhance the resolution of aerial image down to about 0.1 μm isolated line in clear-field mask. With transmittance $T = 35\%$ of the 0.1-μm isolated line as embedded layer, the optimized width of scattering bars is 0.085 μm, the distance between Cr scattering bar and 0.1 μm isolated line is 0.205 μm, and DOF is 0.53 μm under the optimized quadrupole illumination with 0.51/0.27 ($\sigma_{\text{offset}}/\sigma_{\text{radius}}$). Compared to transmittance 5 and 15% of embedded layer, the negative and positive factors of mask error enhancement factor (MEEF) could be kept in the range of -2 to $+2$ for isolated lines wider than 80 nm at transmittance 35%, assisted with the 0.085-μm width of Cr scattering bars. © 2001 Published by Elsevier Science B.V.

Keywords: High transmittance; Scattering bar; Mask error enhancement factor; Attenuated phase-shifting mask; Quadrupole illumination

1. Introduction

Due to the delay in the development of 193 nm ArF resists and exposure tools, 248-nm KrF lithography could be considered to be the most promising technology for 120-nm [1] or even 100-nm devices. In order to obtain good imaging performance of sub-130-nm pattern, the NA/coherence optimization [2] and resolution enhancement techniques such as off-axis illumination (OAI) and attenuated phase-shifting mask (AttPSM) have been investigated [3]. As the pattern size comes closer to the resolution limit of the imaging system, the control of process window becomes more difficult. However, focusing on 100-nm devices, the evaluation of enhancement of depth-of-focus (DOF) with OAI and normal transmittance AttPSM revealed a limit [4]. Thus, in terms of enhancing the resolution of aerial image, the high transmittance AttPSM, used for the contact hole [5], would improve the process window of sub-100 nm line pattern in the clear-field masks, effectively.

The novel high transmittance ($T \sim 35\%$) $AlSi_xO_y$ embedded layer of AttPSM has been presented

*Corresponding author.
E-mail address: loong@cc.nctu.edu.tw (W.-a. Loong).

elsewhere [6]. The target of this paper is to study the effect of high transmittance AttPSM, assisted with Cr scattering bars on the resolution of aerial image and process window of line pattern. The process window of multi-pitch line patterns would be simulated and optimized through NA, illumination shape and bias of mask pattern. Mask error enhancement factor (MEEF) is another issue for sub-130-nm pattern and has been also studied in this paper.

2. Experimental

All experiments were done with lithography simulation software. The lithography simulation software used were Solid-C Ver. 5.52 (Sigma C) and Prolith Ver. 6.02 2D (Finle). The exposure and resist conditions in 248 nm were three NAs, 0.55, 0.6 and 0.65, quadrupole illumination, Shipley chemically amplified positive photoresist UV5, resist thickness of 0.3–0.4 μm and SiO_xN_y BARC thickness of 0.055 μm. The DOF was decided under the conditions, 10% exposure latitude, vertical angle of line pattern between 80 and 92°, and resist thickness loss smaller than 10% in 248-nm lithography. The value of 0.3 for the threshold intensity was used to determine the critical dimensions (CDs) at a wide variety of line pitches. The substrate is a Si wafer. The process window was compared among three different transmittances, 5, 15 and 35% embedded layer of AttPSM for line patterns. The MEEF is defined as the ratio of wafer CD error over absolute value of mask CD error:

$$\text{MEEF} = \frac{\Delta CD_{\text{wafer}}}{|\Delta CD_{\text{mask}}|}$$

The negative or positive wafer CD errors cause the negative or positive factors of MEEF. Here, the mask CD error was taken as 4 nm to evaluate the effects of NA and transmittance of AttPSM on MEEF.

3. Results and discussion

3.1. The effect of transmittance of embedded layer of AttPSM on the resolution of aerial image of line pattern

The variation of light intensity of aerial image at the center of line for various linewidths under embedded layer $T = 35\%$, $\lambda = 248$ nm, NA $= 0.65$ and quadrupole illumination of 0.5/0.3 (σ_{offset}/σ_{radius}) is shown in Fig. 1a. When the clear-field mask linewidth was larger than $\sim$1.31 λ/NA ($\sim$0.50 μm), the frequency of line pattern would be doubled. Linewidth 1.31 λ/NA$\sim$0.69 λ/NA (0.50–0.28 μm) started to show the interaction between line patterns. Linewidth less than $\sim$0.69 λ/NA which we defined as linewidth W would generate single resist line on wafer only because the light intensity of aerial image at center of line on mask was smaller than threshold intensity for resist developing on wafer. Linewidth W is the critical linewidth on mask for single line on wafer (CLMSLW). The line pattern showed the similarity to line pattern from shifter-only PSM [7]. This linewidth W (CLMSLW) was fitted to an exponential function as shown in Fig. 1b. Linewidth W was simulated as a function of T of embedded layer for three kinds of quadruple illumination. The fitted function is shown below:

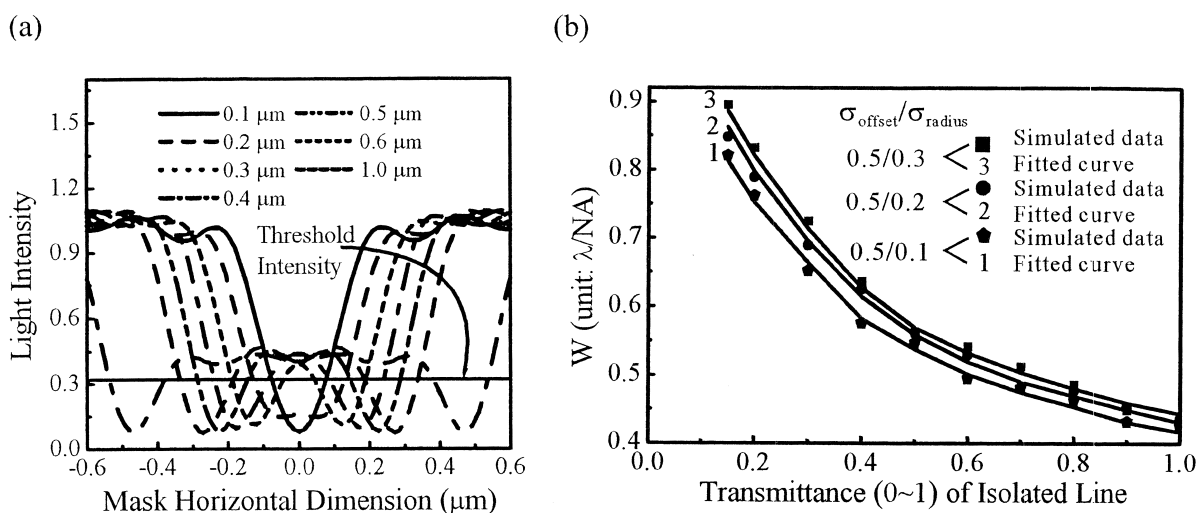$$W = A_0 + A_1 \exp[-(T - 0.3)/X]$$

(a)

(b)

Fig. 1. (a) The aerial images of isolated line for various linewidths under $T = 35\%$ of embedded layer; (b) The marginal linewidth W of isolated line against T (0–1) of AttPSM for three kinds of quadrupole illumination. The fitted curves are also shown.

where W (in units of λ/NA) is the designed CLMSLW, A_0 is 0.383–0.413, A_1 is 0.276–0.296, T (0–1) is the transmittance (not 0–100 $T\%$) of embedded layer and X is 0.322–0.346.

The linewidth smaller than W is suitable for the application of high T AttPSM to obtain single line in resist.

The high transmittance AttPSM could be used to enhance the resolution of isolated lines in clear-field masks, equivalent to the enhancement of DOF, effectively. The development of high transmittance, smaller than 40%, embedded layer of AttPSM is studied here. Compared to normal transmittance ($T < 10\%$) AttPSM, the higher transmittance AttPSM in clear-field masks has higher electric field amplitude with 180° phase-shift for a 0.1-μm isolated line. The stronger interference could be caused by the higher electric field amplitude with 180° phase-shift at the edge of line pattern, thus, the resolution of aerial image of the 0.1-μm isolated line increased with the increasing of transmittance of embedded layer of AttPSM at two values of focus as shown in Fig. 2 at 248 nm. The DOF of the 0.1-μm isolated line would be enhanced. If the opaque Cr scattering bars were placed beside the high transmittance AttPSM pattern, the scattering bars could cause the stronger destructive interference with the zero-order electric field amplitude of main pattern, and the intensity of aerial image at the center of main pattern would be decreased. Thus, the resolution of aerial image of the 0.1-μm isolated line could be also intensified as shown in Fig. 3. The intensity of aerial image of scattering bars was larger than threshold intensity, so it was not imaged. Therefore, the dual enhancements would improve the process window of the 0.1-μm pattern more effectively.

3.2. The enhancement of DOF of the 0.1-μm line with high transmittance AttPSM assisted with Cr scattering bars

For the evaluation of DOF of the 0.1-μm isolated line, the resist thickness is 0.31 μm, decided by the experiment of swing curve of dose-to-resist thickness, and is at the trough of swing curve. In order
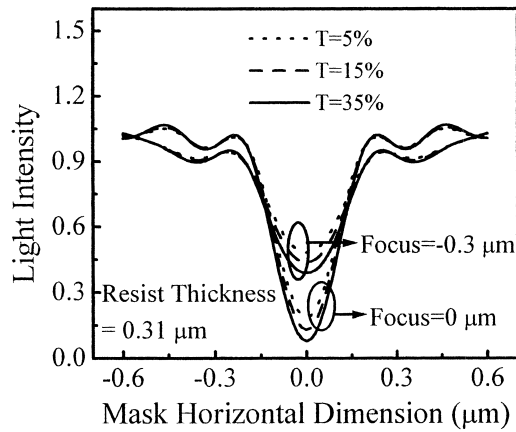
Fig. 2. The resolution of aerial image for the 0.1-μm isolated line increased with the increasing of *T* of embedded layer of AttPSM in clear-field mask at two values of focus at 248 nm.

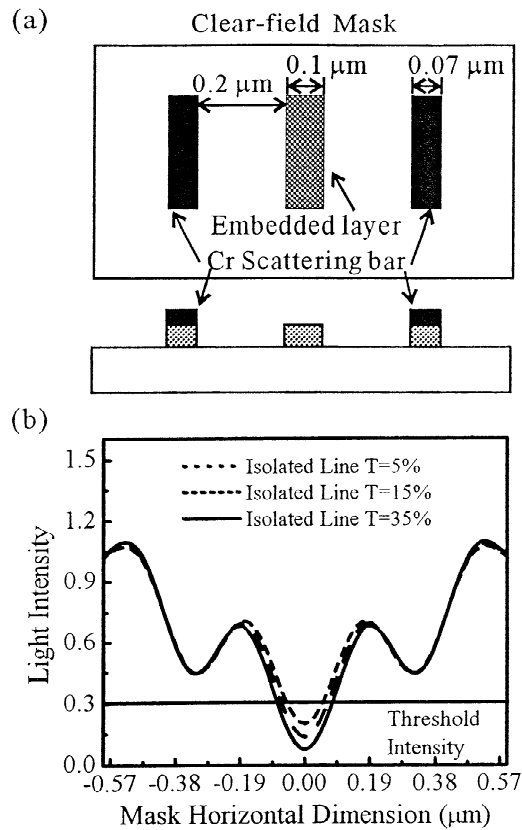Fig. 3. (a) The layout of AttPSM of the 0.1-μm isolated line, assisted with Cr scattering bars; (b) the higher transmittance of embedded layer increasing the resolution of aerial image of the 0.1-μm line at 248 nm.
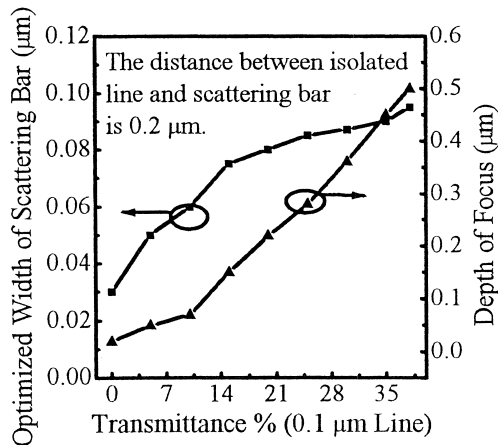
Fig. 4. The effect of transmittance of embedded layer with the optimized width of scattering bars on the DOF of the 0.1-μm isolated line at 248 nm.

to avoid the unwanted side-lobe resist patterns caused by the opaque Cr scattering bars, the width of scattering bars must be optimized, while at same time, the DOF of the 0.1-μm isolated line also has to be improved, effectively. The better distance between isolated line and scattering bar is 0.2 μm. The variation of optimized width of scattering bars and DOF against the transmittance (0–40%) of the 0.1-μm isolated line under NA 0.65 and quadrupole illumination with 0.5/0.2 ($\sigma_{\text{offset}}/\sigma_{\text{radius}}$) is shown in Fig. 4. Because of the limitation of transmittance of embedded layer [6], the optimized width of scattering bars was studied at transmittance 35% of the 0.1-μm isolated line. The exposure conditions were NA$=0.65$ and quadrupole illumination with 0.5/0.2 ($\sigma_{\text{offset}}/\sigma_{\text{radius}}$). The width of scattering bars, larger than 1.1 μm would show the visible side-lobes; however, too narrow scattering bars could not provide enough DOF. The optimized width of scattering bars and distance between scattering bar and main pattern were about 0.085 and 0.205 μm, respectively. These optimized conditions could provide 0.5 μm DOF for the 0.1-μm isolated line as shown in Fig. 5.
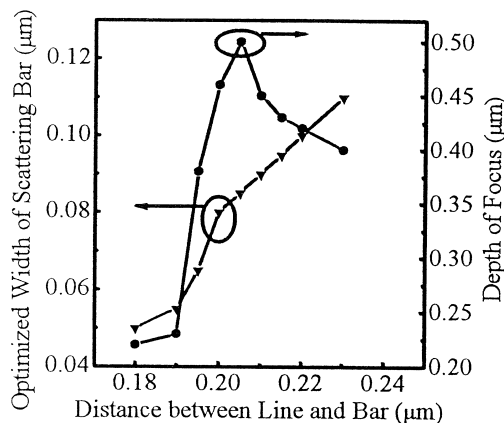

Fig. 5. The effect of distance between scattering bar and line with the optimized width of scattering bars on the DOF of the 0.1-μm isolated line at 248 nm. Transmittance, 35%, NA, 0.65 and quadrupole illumination with 0.5/0.2 ($\sigma_{\text{offset}}/\sigma_{\text{radius}}$).
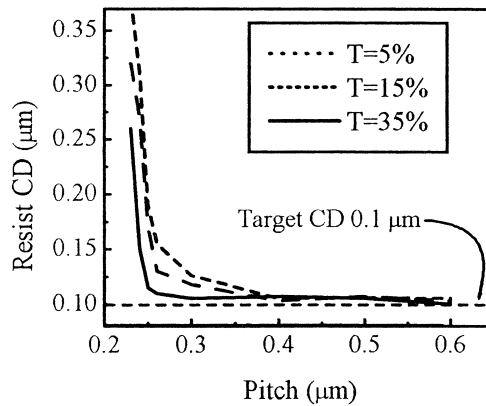
Fig. 6. Compared to 5 and 15%, less optical proximity effect for 0.1-μm line patterns was found at transmittance of 35% and pitches smaller than 0.35 μm.

The analysis mode in Solid-C was used to optimize the quadrupole illumination. The optimized one, 0.51/0.27 for ($\sigma_{\text{offset}}/\sigma_{\text{radius}}$) could provide the better DOF, about 0.53 μm. In contrast to the application of double-exposure technique of alternate phase-shifting and trim masks for the 0.1-μm logic device gate pattern [8], this method could avoid the overlay and light intensity imbalance issue of alternate phase-shifting and trim masks, and provide enough process window.

The optical proximity effect existed evidently for 0.1-μm multi-pitch line patterns. The rule-based optical proximity effect correction, assisted with bias and Cr scattering bars was utilized to optimize the linewidth of line patterns to meet the target CD of 0.1 μm. The comparisons of resist CD among $T = 5$, 15 and 35% for multi-pitches were shown in Fig. 6. Compared to 5 and 15%, less optical proximity effect for 0.1-μm line patterns was found at transmittance of 35% and pitches smaller than 0.35 μm; however, CD = 0.1 μm could not be met for pitches smaller than 0.24 μm.
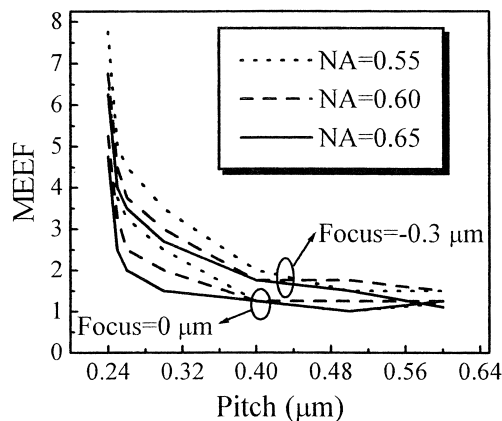

Fig. 7. The comparisons of MEEF of the 0.1-μm line patterns among three NAs, 0.55, 0.6 and 0.65 for pitches from 0.24 to 0.60 μm.
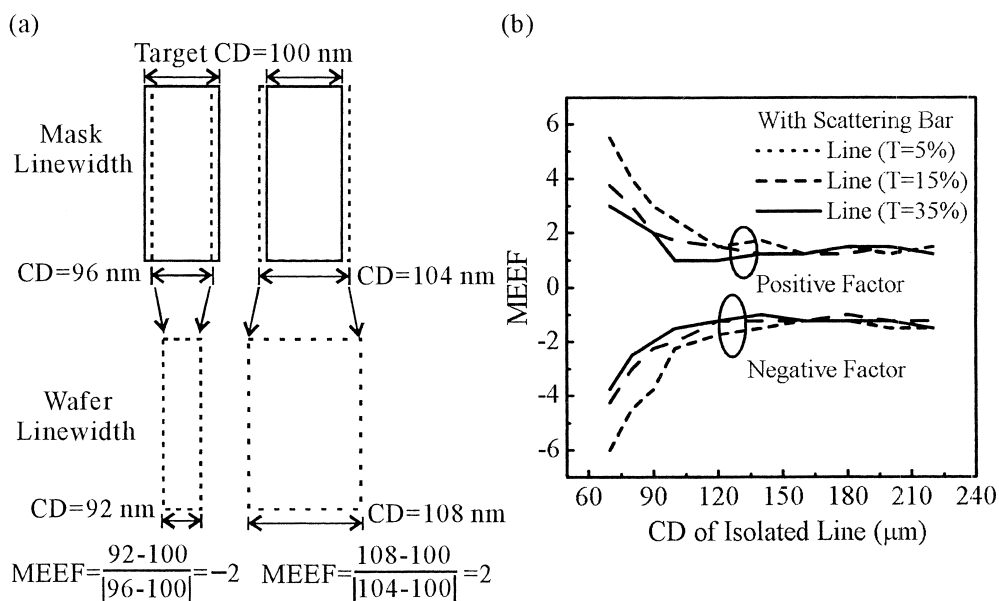
Fig. 8. (a) A schematic illustration of negative and positive factors of MEEF; (b) MEEF could be kept in the range of −2 to +2 for isolated lines wider than 80 nm at transmittance of 35% of the line assisted with Cr scattering bars.

3.3. The evaluation of mask error enhancement factor (MEEF)

For 'linear' imaging, mask CD error (taking into account the reduction factor of the exposure tool) would translate directly into wafer CD error. Thus, a 4-nm CD error on mask linewidth would result in a 4-nm CD error on wafer linewidth. However, for a given exposure tool with particular illumination conditions and resist, the CD error on wafer linewidth might be amplified. Fig. 7 shows the comparisons of MEEF among three NAs, 0.55, 0.6 and 0.65 for 0.1-μm multi-pitch line patterns. The range of pitches is from 0.24 to 0.60 μm. Because the light interference would be stronger for more dense lines, a larger CD variation existed and caused a larger MEEF. A smaller MEEF was obtained for NA 0.65; however, the MEEF was larger than 2 for pitches smaller than 0.25 μm. The schematic interpretation of negative and positive factors of MEEF is shown in Fig. 8a. The negative and positive factors of MEEF could be kept in the range of −2 to +2 for isolated lines wider than 80 nm at transmittance of 35% of line, assisted with Cr scattering bars as shown in Fig. 8b. Accordingly, this technique has the potential to extend 248-nm KrF lithography to 80-nm gate pattern.

4. Conclusions

The optimized width of scattering bars and distance between Cr scattering bar and 0.1-μm line under high transmittance AttPSM and quadrupole illumination are shown. In contrast to the application of double-exposure technique of alternate phase-shifting and trim masks for the 0.1-μm gate pattern, the method can avoid the overlay and light intensity imbalance issue, and improve the process window effectively.

The negative and positive factors of MEEF could be kept in the range of -2 to $+2$ for isolated lines wider than 80 nm at transmittance of line of 35%, assisted with the 0.085-μm width of Cr scattering bars. The technique has the potential to extend 248-nm KrF lithography to the 80-nm gate pattern.

References

[1] S. Nakao et al., Jpn. J. Appl. Phys. Part 1 38 (12B) (1999) 6985.
[2] S. Matsuura et al., Jpn. J. Appl. Phys. Part 1 37 (12B) (1998) 6689.
[3] J.N. Randall, A. Trichkov, J. Vac. Sci. Technol. B 16 (6) (1998) 3606.
[4] I.S. Kim et al., Proc. SPIE 3679 (1999) 872.
[5] J.F. Chen et al., Microlithography World Summer (2000) 12.
[6] C.M. Lin, W.A. Loong, Jpn. J. Appl. Phys. Part 1 39 (12B) (2000) 6801.
[7] K.K.H. Toh et al., Proc. SPIE 1496 (1990) 27.
[8] C.C. Kuo et al., J. Vac. Sci. Technol. B 17 (6) (1999) 3296.